Electronic Supplementary Material (ESI) for Chemical Communications.

In-situ Surface Reconstruction Synthesis of Nickel Oxide/ Nickel Heterostructural Film for Hydrogen Evolution Reaction

Haixin Chen [a], Dongqi Ge [b], Junwei Chen[a], Ruchun Li [a], Xiaofeng Zhang [a], Tongwen Yu [a], Yi Wang [a], Shuqin Song[a,]*

[a] The Key Lab of Low-carbon Chemistry & Energy Conservation of Guangdong Province, School of Chemical Engineering and Technology, School of Materials Science and Engineering, Sun Yat-sen University, Guangzhou, 510275, China

[b] School of Chemical Engineering, Guangdong University of Petrochemical Technology, Maoming, 525000, China

Materials

Ethanamine, N, N-diethyl-, hydrochloride ($C_6H_{15}NHCl$), N, N-Dimethylformamide (DMF), $Ni(CH_3COO)_2 \cdot 4H_2O$, ethanol, carbon cloth (CC) and commercial Ni were received from Aladdin. All the chemical reagents were commercially available and analytical grade, and used without any further treatment.

Synthesis of Ni@CC and NiO/Ni@CC. Electrochemical deposition was carried out by the potentiostatic method in a two-electrode cell. The nickel foam (1.0 cm×2.0 cm) was used as the counter electrode, which was sonicated in 3.0 M HCl for 10 min to remove the possible surface oxide layer. The CC (1.0 cm×2.0 cm) was utilized as the working electrode, which was heated at 400^{o}C for 3 h to enhance its wettability and remove the possible impurities. Ni was electrodeposited on CC (Ni@CC) at -5.0 V in a solution of 95.0 mL DMF and 5.0 mL absolute ethanol including 1.0 mmol (2.488 g) $Ni(CH_3COO)_2 \cdot 4H_2O$ and 1.0 mmol $C_6H_{15}NHCl$ (1.376 g). The different electrodeposition time of 2, 10, 20, and 30 min was investigated and the corresponding samples were labeled as Ni@CC-2, Ni@CC-10, Ni@CC-20, and Ni@CC-30, respectively.

Finally, the above samples were treated by in-situ surface reconstruction through an electrochemical process in a three-electrode system. An Ag/AgCl electrode and a graphite paper (Qingdao Dongkai graphite Co., Ltd.) were respectively used as the reference and counter electrodes at room temperature in 1.0 M KOH solution at 1.4 V

for 100 s to obtain the corresponding NiO/Ni@CC samples. Accordingly, they were labeled as NiO/Ni@CC-2, NiO/Ni@CC-10, NiO/Ni@CC-20, and NiO/Ni@CC-30, respectively.

For comparison reason, Pt/C@CC electrode was also prepared as follows: 5.0 mg Pt/C powders (John Matthey Corp., 20 wt.%), 80.0 μL Nafion® solution (DuPont Company, 5 wt.%), and 920.0 μL absolute ethanol were added into a 2.0 mL centrifuge tube. Then the catalyst slurry was ultrasonicated in an ice bath for 30 min, and the slurry was brushed onto the CC with ~1.0 mg cm^{-2} mass loading of Pt/C.

Physical and chemical characterization. The phase composition and crystal structure were studied by a D-MAX 2200 VPC diffractometer equipped with Cu Kα radiation (40 kV, 26 mA). Morphologies of the samples were examined using Scanning electron microscopy (SEM) and transmission electron microscopy (TEM). SEM and TEM images were taken on a Quanta 400FEG field emission scanning electron microscope and Tecnai G2 F30, respectively. X-ray photoelectron spectroscopy (XPS) tests were performed in an ESCALAB 250 spectrometer. All XPS spectra were corrected using the C 1s line at 284.8 eV, and curve fitting and background subtraction were accomplished. The obtained spectrograms were analyzed employing Xpspeak 41 software.

Electrochemical characterization. Electrochemical measurements were carried out in a conventional three-electrode system at room temperature. A Ni@CC or NiO/Ni@CC

was adopted as the working electrode. An Ag/AgCl electrode and a graphite paper (Qingdao Dongkai graphite Co., Ltd.) were used as the reference and counter electrodes, respectively. KOH solution (1.0 M) was used as the electrolyte.

Linear sweep voltammetry (LSV) was conducted at a scan rate of 5 mV s^{-1} to evaluate the hydrogen evolution reaction (HER) performance. Electrochemical impedance spectroscopy (EIS) analysis was performed using a 5 mV amplitude AC signal in a frequency range from 100 kHz to 10 mHz. The polarization curves were iR-corrected for an ohmic drop obtained from EIS. The reference electrode was calibrated with respect to reversible hydrogen electrode (RHE) according to Equation (1).

$$E_{vsnRHE} = E_{vs\ Ag/AgCl} + 0.098 + 0.059\ pH \quad (1)$$

Current–time (i–t) responses were obtained by chronoamperometric measurements. Cyclic voltammograms (CVs) with various scan rates were used to estimate the double-layer capacitance (C_{dl}).

$$C_{dl} = \triangle j / v \quad (2)$$

Where $\triangle j$ represents evolution of non-Faradaic current density, v is the scan rates.

According to the already reported works, HER proceeds the following processes (Equations (3) - (5)) in alkaline media.[1, 2]

$$\text{Volmer: } H_2O\ (l) + e^- + * \rightarrow H^* + OH^- \quad (3)$$

$$\text{Heyrovsky: } H^* + H_2O\,(l) + e^- \rightarrow H_2\,(g) + OH^-\,(aq) + * \quad (4)$$

$$\text{Tafel: } H^* + H^* \rightarrow H_2\,(g) + 2^* \quad (5)$$

Supplementary Figures

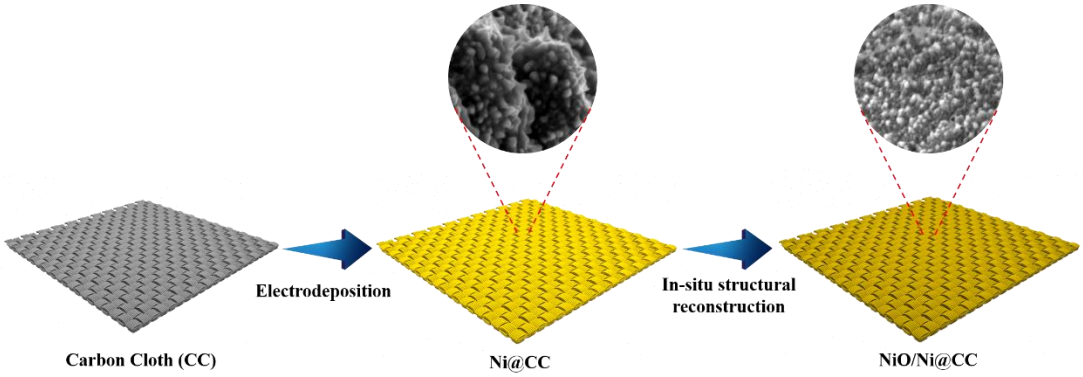

Fig. S1 Schematic of the synthetic process of NiO/Ni@CC.

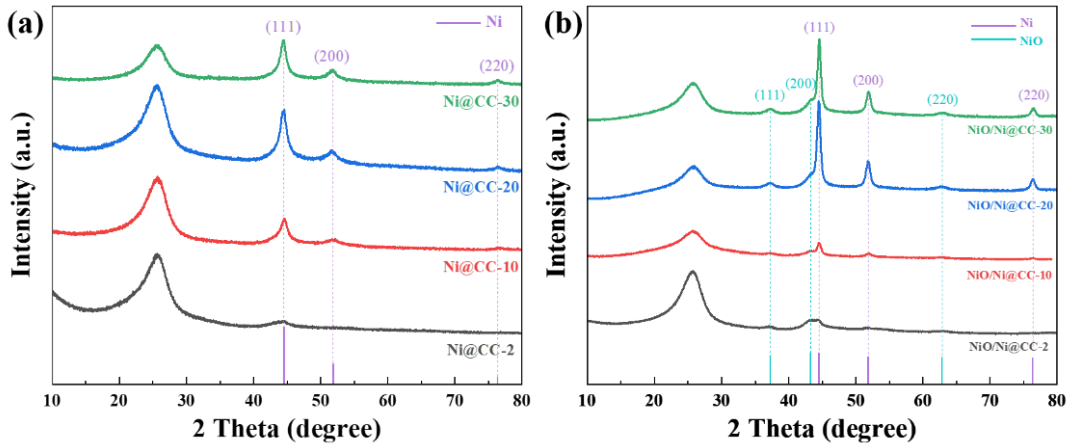

Fig. S2 XRD patterns of (a) Ni@CC and (b) NiO/Ni@CC with different electrodeposition time.

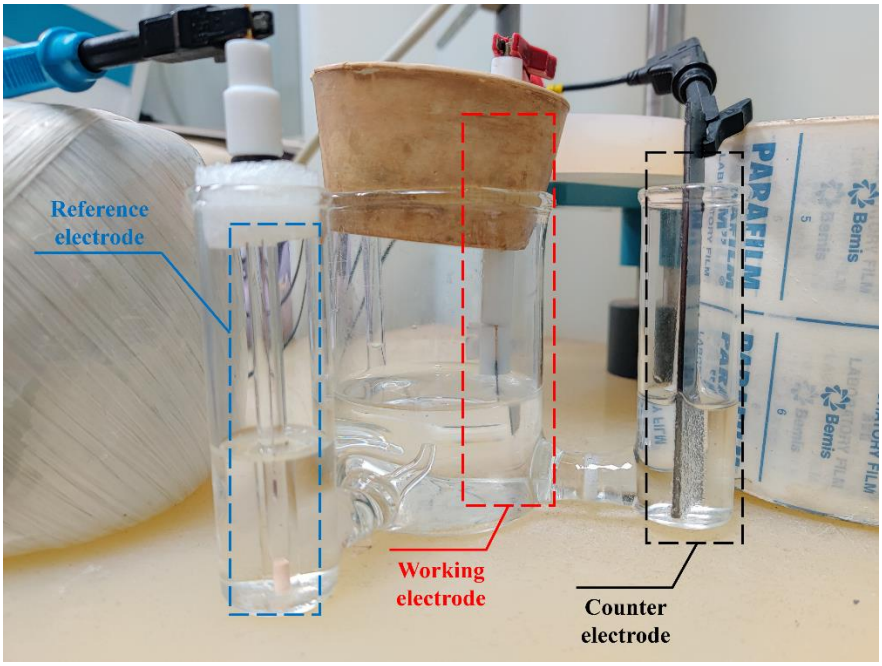

Fig. S3 The optical photograph of the three-electrode electrolysis cell for electrochemical characterizations.

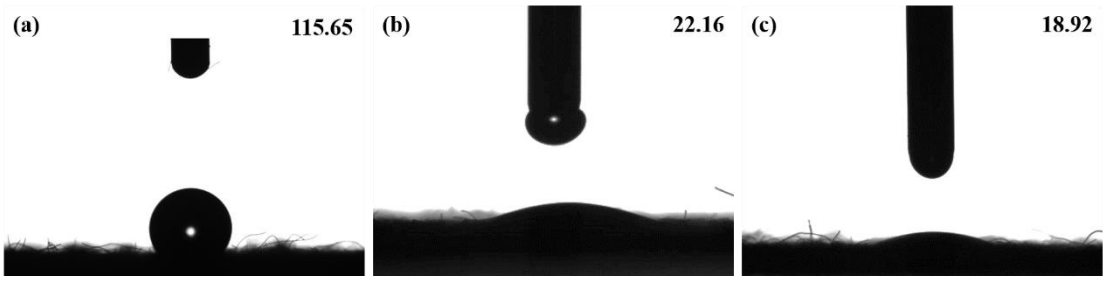

Fig. S4 Contact angle of (a) CC; (b) Ni@CC and (c)NiO/Ni@CC.

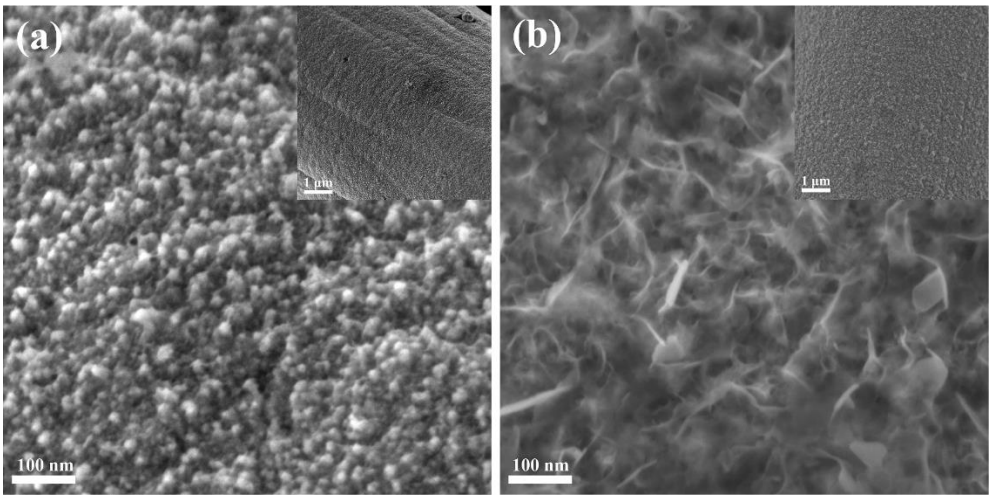

Fig. S5 SEM images (inset is the small magnification image) (a, b) of NiO/Ni@CC-20 before and after HER stability testing at 600 mV (*vs.* RHE) in 1.0 M KOH solution for 10 h.

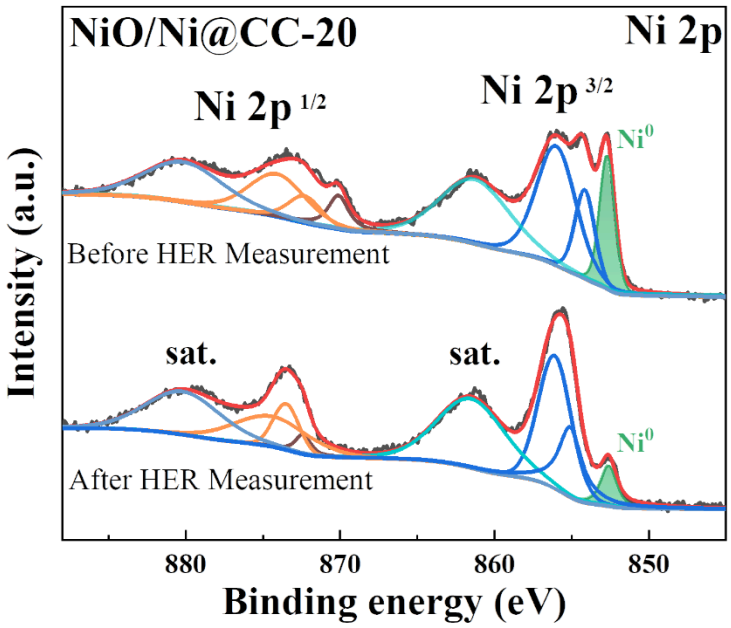

Fig. S6 Ni 2p XPS spectra of NiO/Ni@CC-20 in 1.0 M KOH solution before and after HER stability testing.

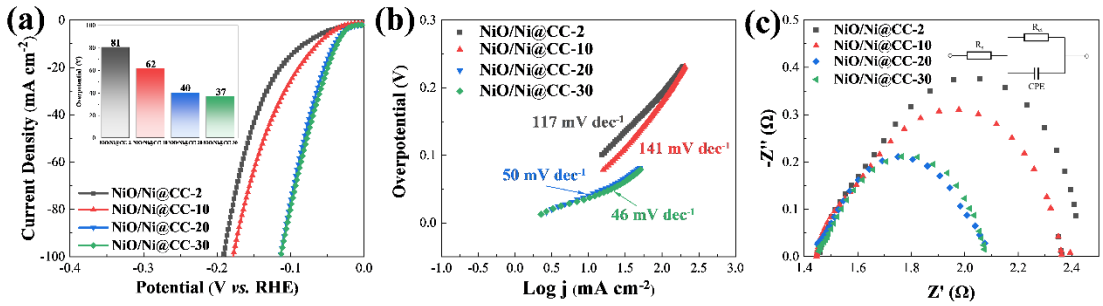

Fig. S7 (a) Polarization curves for NiO/Ni@CC with different electrodeposition time of 2, 10, 20, and 30 min (iR corrected) electrodes at 5 mV s^{-1} (inset is the HER overpotential at 10 mA cm^{-2}); (b) the corresponding Tafel plots; (c) Nyquist plots at a potential of 0.2 V.

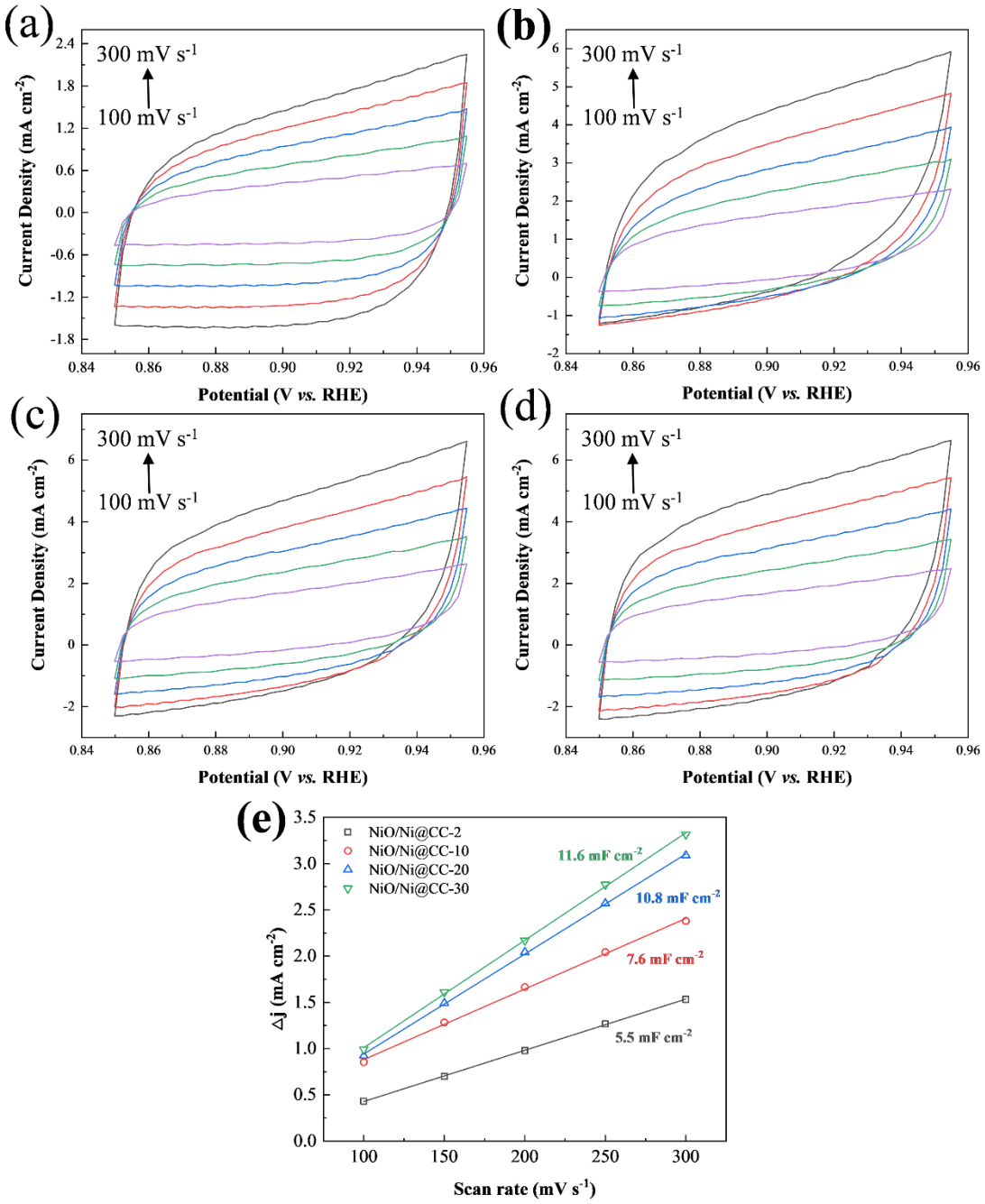

Fig. S8 (a-d) CVs of the NiO/Ni@CC-2, NiO/Ni @CC-10, NiO/Ni @CC-20, and NiO/Ni @CC-30 with different scanning rates from 300 to 100 mV s^{-1}, respectively; (e) their corresponding capacitive current at 0.9 V as a function of scan rate.

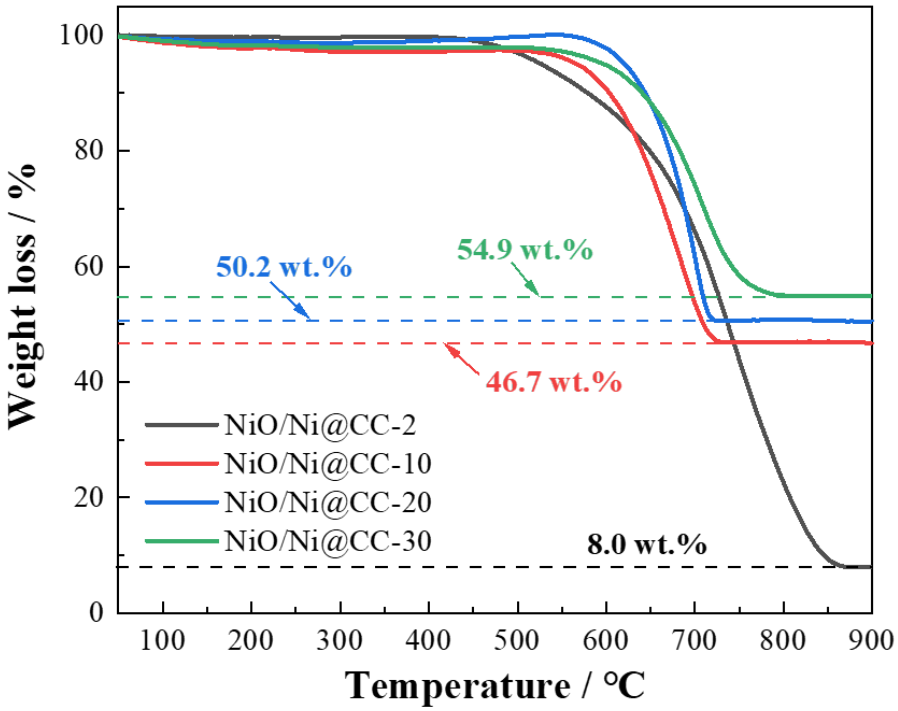

Fig. S9 TG curves of the NiO/Ni@CC.

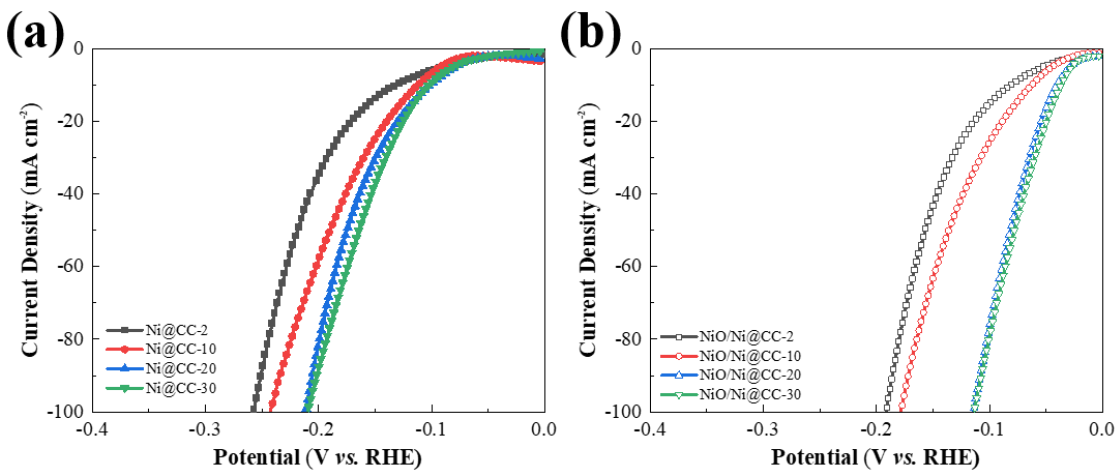

Fig. S10 Polarization curves of Ni@CC (a) and NiO/Ni@CC (b) with different electrodeposition time of 2, 10, 20, and 30 min (iR corrected) in 1.0 M KOH at 5 mV s^{-1}.

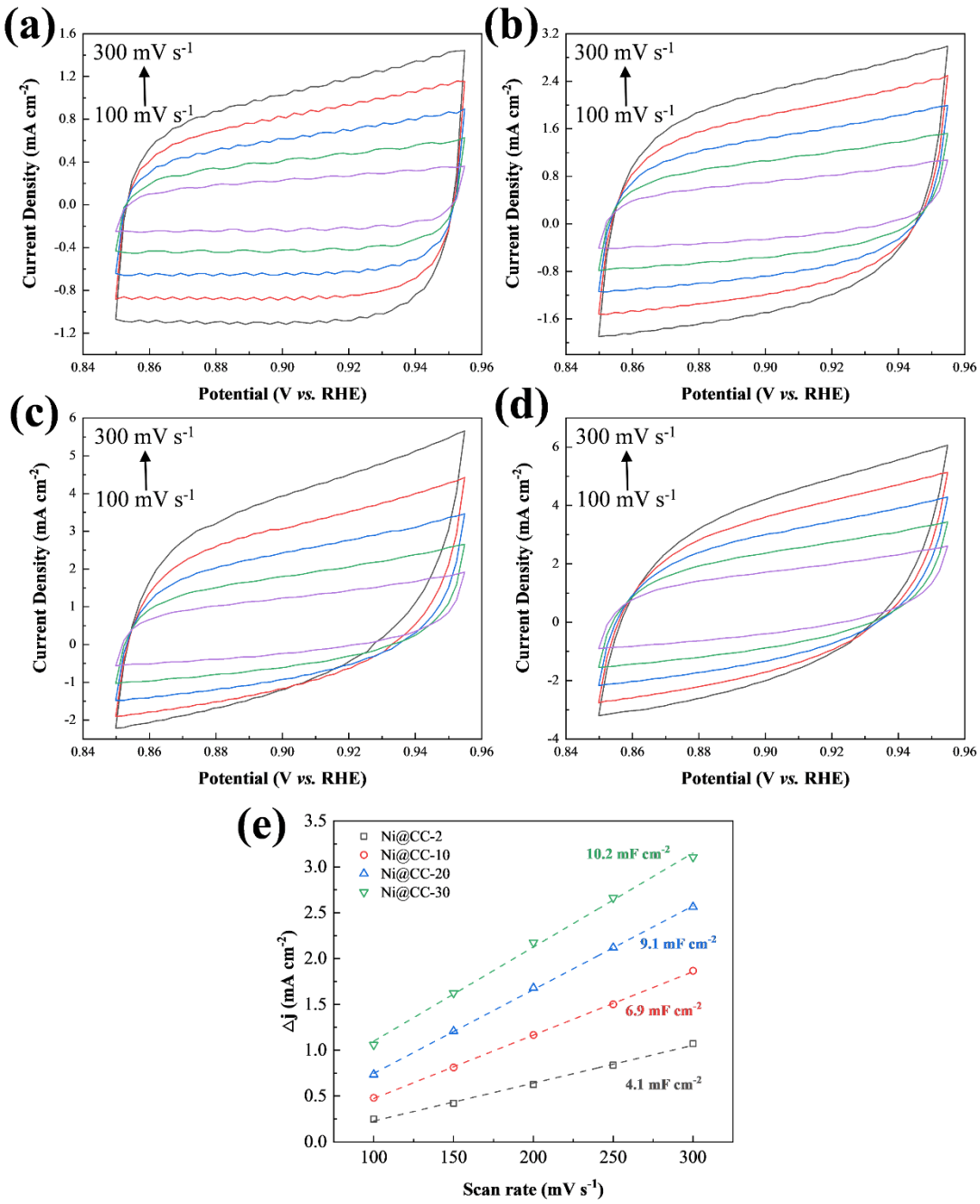

Fig. S11 (a-d) CVs of Ni@CC-2, Ni@CC-10, Ni@CC-20, and Ni@CC-30 with different scanning rates from 300 to 100 mV s^{-1}, respectively; (e) their corresponding capacitive current at 0.9 V as a function of scan rate.

Supplementary Tables

Table S1. The comparison of HER electrocatalytic performance of recently reported Ni based HER electrocatalysts.

Materials	**η at 10 mA cm^{-2}（mV）**	**Tafel slope (mV dec^{-1})**	**Ref.**
NiO/Ni@CC-20 min	**40**	**59**	**This Work**
Ni/PVP-rGO (20)	321	119	[4]
Ni/C_3N_4-0.10	222	128	[5]
Ni_5P_4	~150	53	[6]
Ni_3S_2/NF	223	NA	[7]
Ni/Mo_2C-PC	179	101	[8]
$Ni_{1.2}Co_{0.8}P$	80	51	[9]
NiSe/NF	96	120	[10]
Ni-Co-P nanosheets	107	53	[11]
Se-(NiCo)S/OH nanosheets	103	87	[12]
PO-Ni/Ni-N-CNFs	262	97	[13]
$NiCo_2S_4$ NW/NF	210	59	[14]
Ni/NiO-0.5C	157	99	[15]

REFERENCES

[1] M. Gong, W. Zhou, M.C. Tsai, J. Zhou, M. Guan, M.C. Lin, B. Zhang, Y. Hu, D.-Y. Wang, J. Yang, S. J. Pennycook, B.-J. Hwang, H. Dai, *Nat. Commun.*, 2014, **5**, 1-6.

[2] E. C. Lovell, X. Lu, Q. Zhang, J. Scott, R. Amal, *Chem. Commun.*, 2020, **56**, 1709-1712.

[3] S. L. Medway, C. A. Lucas, A. Kowal, R. J. Nichols, D. Johnson, *J. Electroanal. Chem.*, 2006, **587**, 172-181.

[4] M. Zhiani and S. Kamali, *Electrocatalysis*, 2016, **7**, 466-476.

[5] L. Wang, Y. Li, X. Yin, Y. Wang, A. Song, Z. Ma, X. Qin, G. Shao, *ACS Sustainable Chem. Eng.*, 2017, **5**: 7993-8003.

[6] M. Ledendecker, S. Krick Calderón, C. Papp, H. P. Steinrück, M. Antonietti, M. Shalom, *Angew. Chem. Int. Ed.*, 2015, **54**, 12361-12365.

[7] L.L. Feng, G. Yu, Y. Wu, G.D. Li, H. Li, Y. Sun, T. Asefa, W. Chen, X. Zou, *J. Am. Chem. Soc.*, 2015, **137**, 14023-14026.

[8] Z.Y. Yu, Y. Duan, M.R. Gao, C.C. Lang, Y.R. Zheng, S.H. Yu, *Chem. Sci.*, 2017, **8**, 968-973.

[9] J. Li, M. Yan, X. Zhou, Z.Q. Huang, Z. Xia, C.-R. Chang, Y. Ma, Y. Qu, *Adv. Funct. Mater.*, 2016, **26**, 6785-6796.

[10] C. Tang, N. Cheng, Z. Pu, W. Xing, X. Sun, *Angew. Chem. Int. Ed.*, 2015, **54**, 9351-9355.

[11] E. Hu, Y. Feng, J. Nai, D. Zhao, Y. Hu, X. W. D. Lou, *Energy Environ. Sci.*, 2018, **11**, 872-880.

[12] C. Hu, L. Zhang, Z.-J. Zhao, A. Li, X. Chang, J. Gong, *Adv. Mater.*, 2018, **30**, 1705538.

[13] Z.Y. Wu, W.B. Ji, B.C. Hu, H.W. Liang, X.X. Xu, Z.L. Yu, B.Y. Li, S.H. Yu, *Nano Energy*, 2018, **51**, 286-293.

[14] A. Sivanantham, P. Ganesan, S. Shanmugam, *Adv. Funct. Mater*., 2016, **26**, 4661-4672.

[15] P. Wang, X. Zhang, Y. Wei, P. Yang, *Int. J. Hydrogen Energy*, 2019, **44**, 19792-19804.